Arabian Journal of Chemistry (2021) **14**, 103025

King Saud University

Arabian Journal of Chemistry

www.ksu.edu.sa
www.sciencedirect.com

ORIGINAL ARTICLE

Synthesis, characterization, thermal stability, electrochemical behavior, and antioxidant activity of new oxovanadium(iv) and iron(ii) tetradentate Schiff base complexes

Nadjah Maghraoui [a,d], Djouhra Aggoun [a,*], Brahim Bouzerafa [b], Hamza Bezzi [a], Yasmina Ouennoughi [a], Daniel López [c], Marta Fernández García [c], Ali Ourari [a], Mohammad S. Mubarak [e,*]

[a] *Laboratoire d'Electrochimie, d'Ingénierie Moléculaire et de Catalyse Redox (LEIMCR), Faculté de Technologie, Université Ferhat ABBAS Sétif-1, 19000 Sétif, Algeria*
[b] *Laboratoire de Préparation, Modification et Application des Matériaux Polymériques Multiphasiques (LMPMP), Faculté de Technologie, Université Ferhat ABBAS Sétif-1, 19000 Sétif, Algeria*
[c] *Instituto de Ciencia y Tecnología de Polímeros (ICTP-CSIC), Juan de la Cierva 3, 28006 Madrid, Spain*
[d] *Faculté des Sciences et de la Technologie, Département Génie de l'Environnement, Université Mohamed El-Bachir El-IBRAHIMI, Bordj Bou-Arreridj 34030, Algeria*
[e] *Department of Chemistry, The University of Jordan, Amman 11942, Jordan*

Received 3 November 2020; accepted 15 January 2021
Available online 28 January 2021

KEYWORDS

Oxovanadium(IV) and Iron (II) Schiff base complexes;
Spectroscopic characterization;
Thermal degradation;
Cyclic voltammetry;
Antioxidant activity

Abstract Two new tetradentate oxovanadium(IV) and iron(II) Schiff base complexes have been prepared by the interaction of vanadyl(IV) and iron(III) acetylacetonate with the ligand obtained from the reaction of ethylenediamine and 5′-(N-methyl-N-phenylaminomethyl)-2′-hydroxyacetophenone in methanol. These complexes have been characterized by means of different spectroscopic techniques such as UV–visible, FT-IR, mass spectrometry, and elemental analysis. In addition, thermogravimetric (TG) and differential thermogavemetric analysis (DTG) have been utilized to investigate the thermal stability of these complexes. Results showed that both Schiff base complexes decompose in five consecutive stages, and a mechanism has been proposed for each stage of thermal decomposition. Thermogravimetric analysis has been carried out using four different

* Corresponding authors.
E-mail addresses: aggoun81@yahoo.fr, djouhra.aggoun@univ-setif.dz (D. Aggoun), mmubarak@ju.edu.jo, mmubarak@indiana.edu (M.S. Mubarak).

Peer review under responsibility of King Saud University.

Production and hosting by Elsevier

https://doi.org/10.1016/j.arabjc.2021.103025
1878-5352 © 2021 Published by Elsevier B.V. on behalf of King Saud University.
This is an open access article under the CC BY-NC-ND license (http://creativecommons.org/licenses/by-nc-nd/4.0/).

heating rates of 5, 10, 15, and 20 °C min^{-1}, and the kinetic parameters of these complexes have been calculated using the Kissinger method. Cyclic voltammetry has been employed to examine the electrochemical behavior of the two synthesized complexes in dimethyl sulfoxide (DMSO) at a glassy carbon electrode. Each of these complexes displayed one quasi-reversible single electron transfer peak near 0.255 V vs. saturated calomel electrode (SCE) for the V(V)–V(IV) couple and near −0.690 V vs. SCE for the Fe(III)–Fe(II) redox couples, respectively. Finally, the antioxidant activity of the newly prepared complexes has been investigated using the 2,2-diphenyl-1-picrylhydrazyle (DPPH) free radical scavenging assay. Results revealed that the oxovanadium Schiff base complex exhibits good antioxidant activity.

© 2021 Published by Elsevier B.V. on behalf of King Saud University. This is an open access article under the CC BY-NC-ND license (http://creativecommons.org/licenses/by-nc-nd/4.0/).

1. Introduction

Owing to their interesting physical and chemical properties, Schiff bases continue to play a significant role in coordination chemistry, and to attract the attention of scientists. The first synthesis of a Schiff base was reported by Hugo Schiff (Schiff, 1869) over a century ago. These compounds are formed by reaction of an aldehyde or ketone with a primary amine. This reaction leads to the formation of an azomethine group (—CH═N) or imine function. Recently, this class of materials has attracted researchers and manufacturers for their numerous applications such as catalysis (Vairalakshmi and Princess, 2019), electrocatalysis (Ourari et al., 2012), detection of biomolecules (Gorczyński et al., 2016), and in several forms of drugs in pharmacology (Murtaza et al., 2014), among others.

In inorganic chemistry, Schiff base ligands have been considerably developed and considered as the main chelating agents with most of transition metal ions (Aggoun et al., 2017), due to their stabilization in different oxidation states (Bagherzadeh and Amini, 2010; Asadi et al., 2015). In particular, salen ligands, with NNOO donor sites, are known for their simple preparation, and for coordination to transition metals in their various electronic configurations (Ouennoughi et al., 2017).

Materials derived from Schiff base ligands after coordination with transition metals of the first series, such as V, Cr, Mn, Fe, Co, Ni, Cu, and Zn, have potential applications in the pharmaceutical and medicinal fields (Al-Obiadi, 2012; Manjula and Arul, 2013; De Fátima et al., 2018). Structural variety of these compounds can be very useful for their bioactivity including control of anti-inflammatory response, allergic inhibitors, analgesic, and antioxidant activity among others (Ramadhan et al., 2016; Prakach and Adhikari, 2011; Miloud et al., 2020; Abd El-Halim et al., 2017; Al Zoubi et al., 2017; Elsayed et al., 2017). In addition, knowledge of the electrochemical behavior of these Schiff base complexes in different media is necessary for their different applications (Sungh et al., 2017). The efficiency of these compounds in biological and industrial processes, has stimulated research in the coordination chemistry of oxovanadium complexes and attracted the attention of researchers (Maurya et al., 2015). In this regard, oxovanadium Schiff base complexes have been found to exhibit bioactivities such as enzyme inhibition (Mahroof-Tahir et al., 2005), insulin mimetic (Melchior et al., 1999), and anti-amoebic (Maurya et al., 2003). In addition, these complexes exert antibacterial (Mahalakshmi and Rajavel, 2014), anti-inflammatory (Shukla and Mishra, 2019), and anticancer properties (Abd El-Rahman et al., 2020), and could be useful in catalysis (Rayati and Ashouri, 2012), and for pharmacological applications (Pawar et al., 2013).

As for the chemical coordination of iron with this type of Schiff base ligands, the growing interest for the new synthesized complexes is preferred due to the presence of this element in several biological systems (Surati and Sathe, 2016). On the other hand, and besides their function as model compounds for catalytic systems (Ghazizadeh et al., 2017), like iron Schiff base complexes, which display interesting active nonlinear optical (NLO) chromophores (Elmali et al., 2005), iron complexes act synergistically to increase the biological activities and simultaneously decrease the cytotoxic effects (Hassan et al., 2020). Iron complexes exhibit numerous interesting biological activities including as antibacterial (Abd El-Rahman et al., 2017), antimicrobial (Abd El-Halim et al., 2017), antifungal (Abdallah et al., 2010; Miloud et al., 2020), antioxidant, (Pramanik et al., 2015), antitumor activity (Shi et al., 2020), and anticancer (Uddin et al., 2020). Additionally, iron complexes are currently known to be as good models for catechol oxidase mimicking activity (Basak et al., 2018).

Furthermore, this class of compounds has a potential catalytic activity in reactions such as epoxidation of alkenes and oxidation of alcohols and sulfides (Jacob et al., 1989; Rani and Bhat, 2010; Bagherzadeh and Amini, 2009). Thus, the synthesis of new symmetrical tetradentate Schiff base complexes remains the target of several recent research, which encouraged us to continue our previous work on the synthesis and characterization of the Schiff base complexes of nickel (II) and cobalt (II) (Ourari et al., 2014, 2015). Based on the preceding discussion, we report, herein, the synthesis, characterization, electrochemical, thermal behavior, and antioxidant activity of two new Schiff base complexes of oxovanadium(IV) and iron(II) (Scheme 1).

2. Experimental

2.1. Materials and reagents

All reagents and chemicals used throughout this work were obtained from commercial sources, and were used without further purification. Solvents such as dichloromethane (DCM), methanol (MeOH), acetonitrile (CH_3CN), dimethylformamide (DMF), and dimethyl sulfoxide (DMSO) were of analytical grade and were purchased from Sigma-Aldrich.

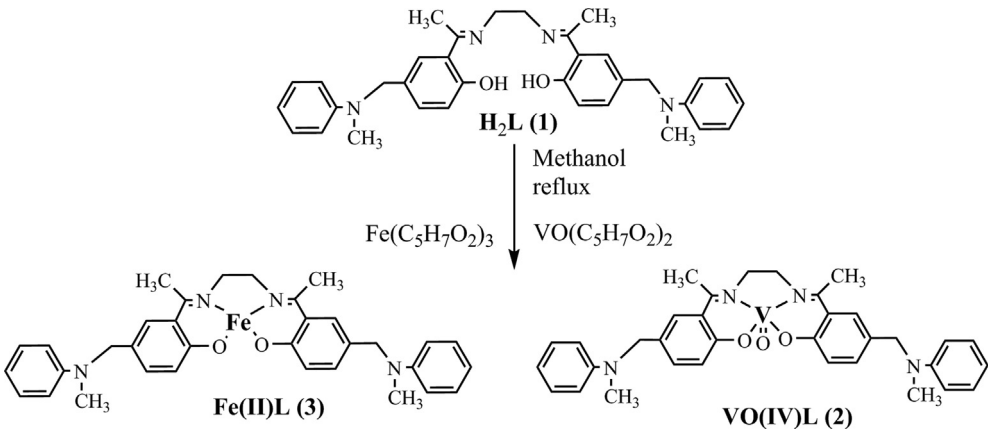

Scheme 1 Synthesis of Schiff base complexes of oxovanadium(IV) and iron(II).

2.2. Instrumentation and measurement

Purity of the iron and oxovanadium complexes was checked by means of thin-layer chromatography (TLC). Elemental analyses were acquired with a Euro EA3000 CHNS-O elemental analyzer (Milian, Italy). Infrared spectra, as KBr disks, of the complexes were recorded with a Perkin-Elmer 1000 spectrophotometer in the range of 400–4000 cm^{-1}, whereas electronic spectra were obtained with a UNICAM UV − 300 instrument with DMSO solutions (1-cm cell) using quartz cuvettes. High-resolution mass spectra (HRMS) were acquired by electrospray ionization-mass spectrometry (ESI-MS) with the aid of a Bruker APEX-2 instrument. Thermal stabilities (TG and DTG) of the prepared complexes were studied with the aid of a TA Instruments TGA Q500 thermal analyzer in a dynamic mode. Heating was performed under dry nitrogen atmosphere purging at a flow rate of 60 mL min^{-1} in the temperature range of 20–950 °C; samples were subjected to dynamic thermogravimetric experiments at heating rates of 5, 10, 15, and 20 °C min^{-1}. Cyclic voltammetry experiments were carried out in a one-compartment (undivided) cell using a Voltalab 40 (PGZ 301) potentiostat-galvanostat, equipped with a PC with Volta Master 4 software. We used a circular planar glassy carbon working electrode with a 3.0-mm in diameter, whereas a coil of platinum wire served as the auxiliary (counter) electrode. Dimethyl sulfoxide, dimethylformamide, dichloromethane and acetonitrile were employed as solvents, and tetra-*n*-butylammonium perchlorate (TBAP) as a supporting electrolyte. All potentials cited in this paper are given with respect to the saturated calomel electrode (SCE).

2.3. Procedure for testing antioxidant activity

Antioxidant activity of the Schiff base ligand **H_2L**, the oxovanadium **(IV) (VO(IV)L)** (**2**), and iron**(II)** Fe(II)L (**3**) complexes was studied in a solution of 2,2-diphenyl-1-picrylhydrazyle (DPPH) using UV–vis spectrometry according to a published procedure (Blois, 1958). Briefly, 0.5 mL of 0.1 mM DPPH solution prepared in methanol was added to 1.5 mL of each solution of the samples at different concentrations. The mixture was stirred and left at room temperature for 30 min. The decrease in absorbance was measured at 517 nm. A lower absorbance of the reaction mixture indicates increased free radical scavenging activity. We calculated the percentage of the DPPH free radical scavenging activity using the following equation:

$$\text{DPPH scanvenging activity} = \left(\frac{\text{Abs}_{\text{control}} - \text{Abs}_{\text{sample}}}{\text{Abs}_{\text{control}}}\right) \times 100$$

where $\text{Abs}_{\text{control}}$ and $\text{Abs}_{\text{sample}}$ are the absorbance at 517 nm of DPPH radical without and with tested compounds, respectively. IC_{50}, which is the concentration of the compounds for trapping DPPH radicals at 50%, was determined by extrapolation from the plot of the DPPH trapping activity as a function of the concentration of the compound.

2.4. Synthesis of oxovanadium(IV) and iron(II) complexes

The NNOO tetradentate Schiff base ligand **H_2L** (**1**) was synthesized according to the method described in a previous paper (Ourari et al., 2014). Synthesis of the VO(IV) and Fe(II) complexes, **2** and **3,** was accomplished by reaction of each of the two metal salts of acetylacetonate (**V** and **Fe**) with the ligand in a 1:1 M ratio according to the following procedure: For **2**, a solution of 0.265 g (1.0 mmol) of vanadyl(IV) acetylacetonate in 20 mL of methanol was added dropwise to a methanol solution (20 mL) of 0.534 g (1.0 mmol) of **1**, the stirred mixture was refluxed for 5 h, and the reaction progress was monitored by using thin-layer chromatography (TLC). After the completion of reaction, the green precipitates was filtered, washed with diethyl ether, and dried in vacuum to afford 0.234 g of the vanadium complex **2** (54% yield). The same exact procedure was employed for the synthesis of **3**; for this, 0.534 g (1.0 mmol) of **1** in 20 mL of methanol, and 0.284 g (1.0 mmol) of Fe(III) acetylacetonate in 20 mL of methanol were used. At the end of the reaction, the brown complex **3** (0.284 g, 48%) was obtained. For **VO(IV)L** (**2**): Anal. Calc. for $C_{34}H_{36}N_4O_3V$ (M = 599.61 g mol^{-1}): C 68.10; H 6.05; N 9.34, Found: C 68.22; H 5.70; N 10.38%. **UV–Vis.** (DMSO): λ_{max1} (313 nm), and λ_{max2} (412 nm). **FT − IR** (KBr pellet, cm^{-1}): 2800–3120 (w, C—H aliphatic and aromatic), 1593 (s, C=N), 1293 (m, C—O), 934 (m, V=O), 530 (m, V—O), 431 (m, V—N). **HRMS** (ESI) *m*/*z*: calcd. for $C_{34}H_{36}N_4O_3V$ $[M]^+$ 599.22270, found 599.22224. For **Fe(II)L** (**3**): Anal. Calc. for $C_{34}H_{36}N_4O_2Fe$ (M = 588.52 g mol^{-1}): C 69.39; H 6.17; N 9.52 Found: C 68.65; H 6.18; N 9.11%. **UV–Vis**. (DMSO): λ_{max1} (307 nm),

λ_{max2} (419 nm) and λ_{max3} (500 nm). **FT–IR** (KBr pellet, cm^{-1}): 2800–3100 (w, C—H aliphatic and aromatic), 1597 (s, C═N), 1236 (m, C—O), 512 (m, Fe—O), 415 (m, Fe—N). **HRMS** (ESI) *m/z*: calcd. for $C_{34}H_{36}N_4O_2Fe$ $[M]^+$ 588.21877, found 588.21866.

3. Results and discussion

3.1. Chemistry

Synthesis of the Schiff base ligand was carried out according to a previously published procedure that involved condensation of 5′-(N-methyl-N-phenylaminomethyl)-2′-hydroxyacetophenone with ethylenediamine (Ourari et al., 2014). Treatment of vanadyl(IV) and iron(III) acetylacetonate with an equivalent quantity of the Schiff base ligand **H_2L**, in refluxing methanol, led to the formation of the corresponding Schiff base complexes **VO(IV)L** (**2**) and **Fe(II)L** (**3**) as shown in Scheme 1. Prepared complexes are stable in air, insoluble in water, but easily soluble in DMF and DMSO. Structures of these complexes have been confirmed by several spectroscopic techniques including UV–Vis, FT–IR, and mass spectrometry, and by elemental analysis; mass spectra of the synthesized complexes are in complete agreement with the assigned structures and showed the expected molecular ions (M^+) as suggested by their molecular formulas. In addition, obtained values in elemental analysis are in good agreement with those calculated.

3.2. Spectral studies

3.2.1. UV–Vis and IR spectroscopies

The electronic absorption spectrum of the Schiff base complexes of iron (II) (Fig. 1**A**) and oxovanadium (IV) (Fig. 1**B**) were recorded at room temperature in 10^{-5} M DMSO solutions in the ranges of 270–750 nm and 280–800 nm, respectively. Oxovanadium and iron Schiff base complexes displayed absorption bands observed in the UV region at λ_{max1} = 307 nm and 313 nm, respectively. We attributed these bands to n-π* transitions of the azomethine function (Sasmal et al., 2008). The Schiff base complexes of oxovanadium and iron exhibit absorption bands at λ_{max1} = 307 nm and 313 nm, respectively. Charge transfer bands were also observed in the electronic spectra of **2** and **3** at λ_{max2} of 419 nm and 412 nm, respectively. These bands correspond to the ligand-to-metal charge transfer (LMCT) in **2**, and to metal-to-ligand charge transfer (MLCT) in **3** (Han et al., 2012). In the case of **2**, the shoulder, which appeared at around 389 nm, can be attributed to the LMCT (Bikas et al., 2013). As for the iron complex**,** the weak-energy absorption band observed at 500 nm is probably due to the d-d transitions, confirming its coordination with the ligand.

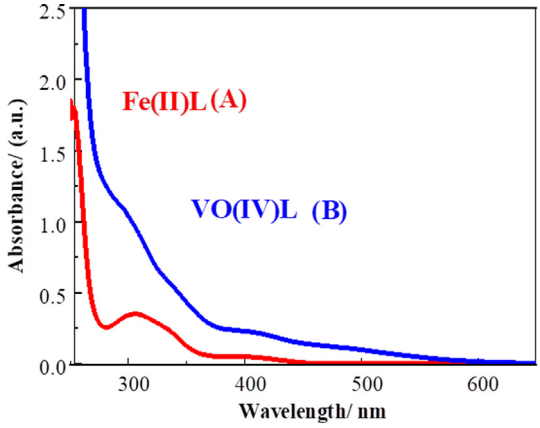

Fig. 1 The UV − Vis spectra (**A** and **B** in 10^{-5} M in DMSO) and IR spectra (**C** and **D**) of the **Fe(II)L** and **VO(IV)L** complexes, respectively.

IR spectra of the oxovanadium and iron complexes, shown in Fig. 2, exhibit several absorption bands in the region of 400–4000 cm^{-1}, which are in good agreement with their proposed structures. These spectra show several weak bands for the aromatic and aliphatic C—H stretching vibration in the region 2800–3100 cm^{-1}. Comparison of the spectroscopic data of the two complexes with those of the Schiff base itself (Ourari et al., 2014) showed a shift in stretching frequencies of the C═N bond from 1616 to 1597 cm^{-1} for **2** and 1593 cm^{-1} for **3**, thus, confirming complexation with the metal ions. This bathochromic shift could be due to the formation of metal-ligand bonds through coordination of oxygen and nitrogen atoms with the metal center, because of the increase in electron delocalization through the newly coordinated metal center (Conley, 1966). Strong absorptions bands in the 1300–1450 cm^{-1} region are attributed to the C═C aromatic stretching. In addition, the absorption band $\upsilon_{(C\text{-}O)}$ moved towards higher wavenumbers (1293 and 1236 cm^{-1}) for **2** and **3**, respectively, indicating coordination of these two metals with the ligand. Furthermore, new weak bands at 530 and 431 cm^{-1} are assigned to V—N and V—O in **2**, whereas the weak bands at 512 and 415 cm^{-1} are attributed, respectively, to Fe—N and Fe—O in **3**, which is in agreement with the literature (Percy and Thornton, 1972). Furthermore, in the IR spectrum of **2**, the ν (V═O) is also observed at 934 cm^{-1}, the presence of this band in this region is in agreement with similar vanadium Schiff base complexes (Kolawole and Patel, 1981; Lu et al., 2011).

3.2.2. Mass spectrometry

A FAB- mass spectrum of the synthesized complexes and their main fragments are given in Fig. 3, whereas the fragmentation pattern is displayed in Scheme 2. For the oxovanadium complex **2**, in addition to the main signal corresponding to the molecular weight of the complex, which appeared at 599.2224, we observe the following major signals whose attributes are illustrated in Scheme 2. The peak at *m/z*: 493.1573 is attributed to $C_{27}H_{28}N_3O_3V^{\bullet+}$ with the loss of the N-methylaniline group, while the peak at 193.5456 is ascribed to the deprotonated fragment $C_{14}H_{11}N^{\bullet+}$. The fragment of *m/z* 135.0807 could be due to the fragment ($C_7H_7^{+}$ + 2Na). For the iron(II) complex **3**, the signal at *m/z* 588.2168 is characteristic of the molecular ion $[M]^+$. In addition, another signal at *m/z*: 482.1511 could probably correspond to the formula of $C_{27}H_{28}N_3O_2Fe^{\bullet+}$. The presence of a fragment at *m/z*: 1177.4346 suggests the presence of a binuclear form of the complex ($C_{68}H_{72}N_8O_4Fe_2$).

3.3. Thermal analysis

To determine the thermal stability of the two prepared complexes **2** and **3**, we performed thermogravimetric analysis (both

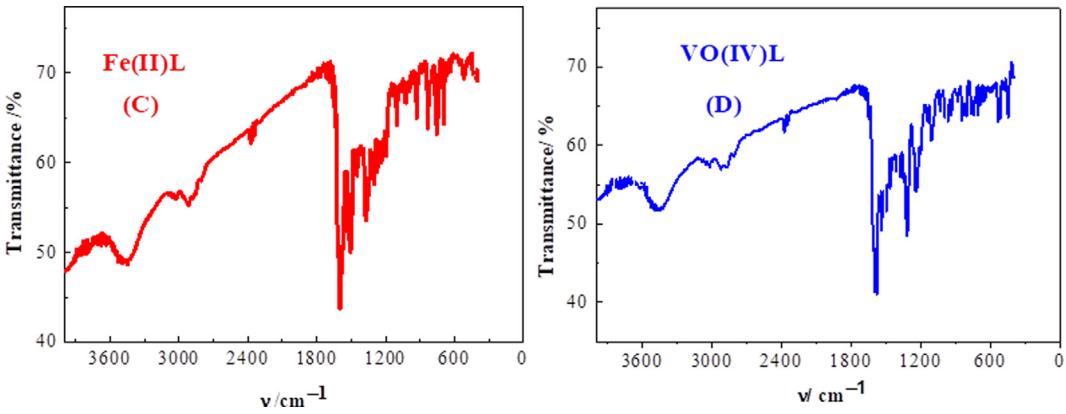

Fig. 2 IR spectra (**A** and **B**) of the **Fe(II)L** and **VO(IV)L** complexes, respectively.

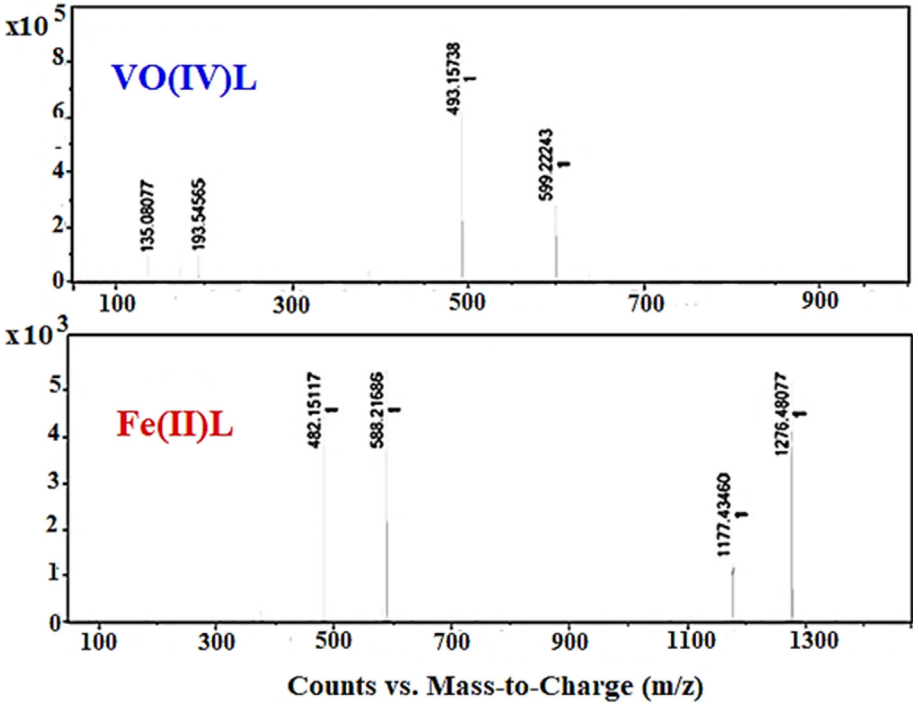

Fig. 3 Mass spectra of oxovanadium and iron Schiff base complexes.

TG and DTG). This analysis plays an important role in the study of thermal stability of complex metallic Schiff bases. These experiments were carried out by increasing the temperature from 50 to 950 °C at a rate of 10 °C min^{-1} under a nitrogen atmosphere. Depicted in Fig. 4 are the TG / DTG thermograms for the two complexes, which showed weight loss in the temperature range of up to 150 °C (First step of degradation process), indicating the absence of water molecules in the two materials (Anthonysamy and Balasubramanian, 2005). For the oxovanadium complex **2**, the thermograms TG and DTG reveal five different stages of decomposition (Yaul et al., 2013). TG curve indicates a mass loss of 9.75% (calculated 10.02%) between 75 and 150 °C attributed to the loss of the four methyl groups present in the structure of this complex, and the maximum weight loss occurs at 135 °C as shown by the corresponding DTG thermograms. In the temperature range of 150–190 °C, a mass loss of 14.95% (calculated 15.19%), (DTG peak observed at 166 °C) which corresponds to elimination of the aniline group (C_6H_5N) was observed. The same group (C_6H_5N) was eliminated in the third stage of decomposition in the temperature range of 190–330 °C, with a DTG peak observed at 237 °C.

The complex undergoes further decomposition in the range of 330–510 °C with a mass loss of 4.45% (calculated 4.67%), and with a DTG peak observed at 425 °C, which could be assigned to the loss of two methylene groups ($2CH_2$). The last step in the temperature range from 510 to 940 °C was characterized by a mass loss of 12.61% (calculated 13.35%). The coordinated moiety $C_4H_4N_2$ is eliminated at 695 °C according to the DTG peak, leading to the final residue of 56.63% (calculated 58.42%), which can probably be attributed to the removal of the stable vanadium monoxide accompanied by

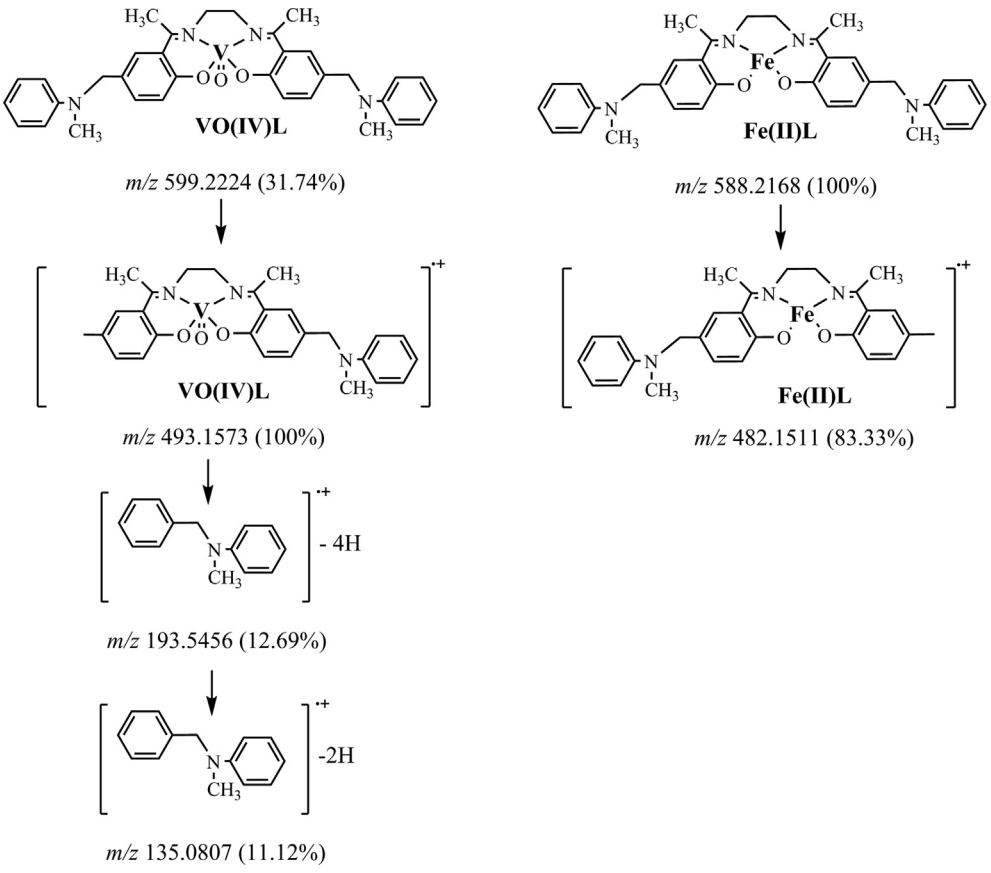

Scheme 2 Proposed fragmentation of **Fe(II)L** and **VO(IV)L** complexes.

two phenolate groups (Asadi et al., 2015; El-Shafiy and Shebl, 2019).

Thermograms (TG) of the iron complex **3** also show five stages of decomposition. The first stage was observed in the temperature range of 75–185 °C, and accompanied by a mass loss of 9.67% (calc. 10.21%). This step is characterized by a peak at 150 °C in the DTG, which can be attributed to the loss of four methyl groups of the ligand as shown in Scheme 3. In the temperature range of 185–330 °C, the complex loses two phenyl groups as indicated by a mass loss of 25.95% (calc. 26.20%); a DTG peak at 240 °C. characterizes this step. The third stage occurs in the temperature range of 330–525 °C with a DTG peak observed at 476 °C, corresponds to a mass loss of 9.68% (calc. 9.52%); this can be attributed to the removal of the $C_2H_4N_2$ group. This stage was followed by a mass loss of 12.51% (calculated 13.60%) in the range 525–660 °C, with a DTG peak at 610 °C, due to loss of $C_4H_4N_2$. The last step was observed in the temperature range of 660–940 °C, and accompanied by a mass loss of 14.95% (calculated 15.19%), attributed to the elimination of an oxygen atom, leading to a stable residue of FeO with two phenyl groups (Zayed et al., 2014).

3.4. Kinetic studies

Based on the thermogravimetric results, we carried out a kinetic study using four heating rates: 5, 10, 15, and 20 °C min^{-1},and the corresponding TG/DTG curves are shown in Fig. 5 (A, B, C, and D). The kinetic thermal decomposition parameters of the two prepared complexes (the activation energy E, and the pre-exponential factor A) are calculated using the Kissinger method according to the following equation (Kissinger, 1957):

$$ln\left(\frac{\beta}{T^2_{max}}\right) = \left\{-ln\left(\frac{E}{RT_{max}}\right) + ln\left[n(1-\alpha_p)^{n-1}\right]\right\} - \frac{E}{RT_{max}} \quad (1)$$

where $\beta$is the heating rate (°C min^{-1}), α is the conversion which is equal to $(1 - w/w_0)$, w/w_0 is the mass loss in %, w_0 and w are the mass of the material at the time zero and t, respectively, and T_{max}, is the temperature that corresponds to the maximum of $d\alpha/dT$. This kinetic method provides a single E value for each reaction step. The plot of $\ln\left(\beta/T^2_{max}\right)$versus $(1/T_{max})$gives a straight line with a slope equal to −E/R as shown in Fig. 6 (A and B). Listed in Table 1 are the obtained activation energies E, and the pre-exponential factors A of each step.

3.5. Cyclic voltammetric behavior of *2* and *3*

Electrochemical measurements such as the anodic (E_{pa}) or cathodic (E_{pc}) peak potentials, the potential difference ($\Delta E_p = E_{pa} - E_{pc}$), and the half-wave potential $E_{1/2}$ of a reversible redox process carried out in dimethyl sulfoxide (DMSO). In this context, the cyclic voltammetric behavior of the

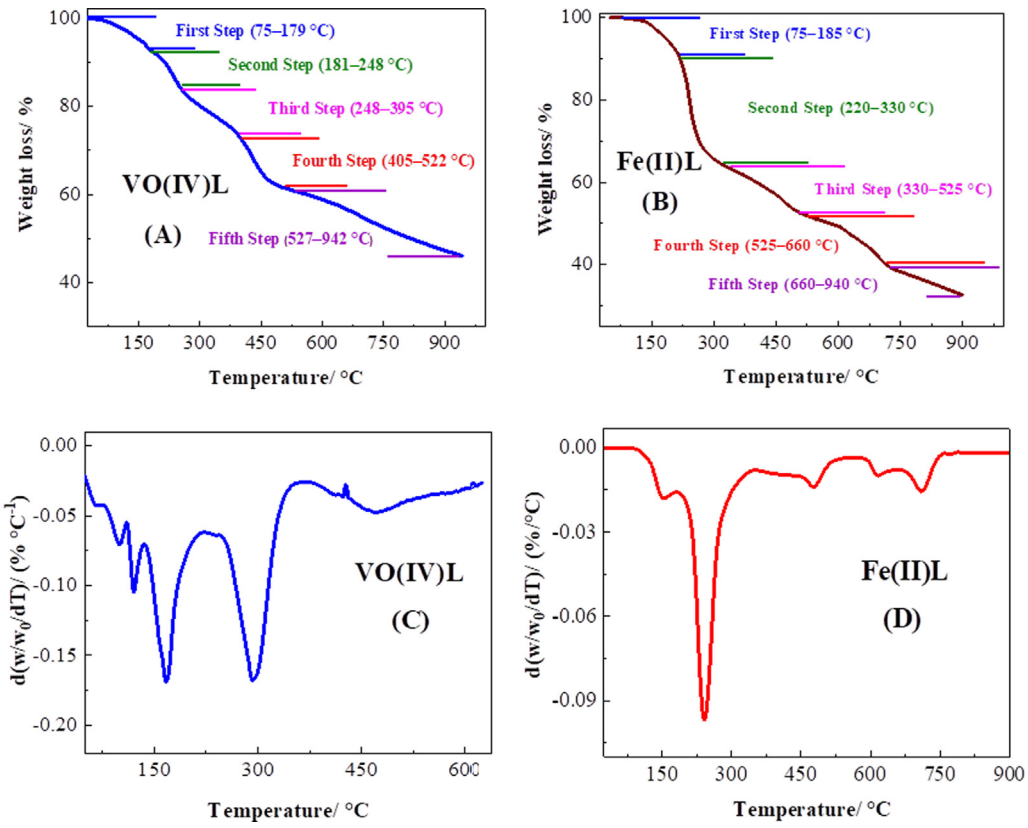

Fig. 4 TG (**A, B**) and DTG (**C, D**) thermograms of **VO(IV)L** and **Fe(II)L** complexes performed at 10 °C min^{-1} under nitrogen atmosphere.

Schiff-base complexes **2** and **3** at a glassy carbon electrode (GC), using tetra-*n*-buthylammonium perchlorate (TBAP) in DMSO was investigated. Displayed in Fig. 7**A** and Fig. 8**A**, are cyclic voltammograms recorded at a scan rate of 100 mV s^{-1} for reduction of 1.0 mM solutions of the complexes **2** and **3** in oxygen-free DMSO containing 0.10 M of TBAP at freshly polished glassy carbon electrodes. These cyclic voltammograms were recorded in the potential ranges from 0.0 to +0.60 V and from −0.30 to −1.00 V versus SCE for **2** and **3**, respectively. The important characteristics of the cyclic voltammogram of **2** is the reversible V(V)–V(IV) redox couple (Kianfar and Mohebbi, 2007) with a cathodic peak potential (E_{pc}) of +0.211 V, an anodic peak potential (E_{pa}) of +0.291 V, and a peak separation ($\Delta E_p = E_{pa} - E_{pc}$) of 80 mV, and the ratio between anodic and cathodic currents (ip_a and ip_c) is close to one. The half-wave potential ($E_{1/2}$) calculated as the average of the cathodic (Ep_c) and anodic (Ep_a) peak potentials is 0.251 V vs. SCE.

We have investigated the effect of scan rate on electrochemical behavior of **2** with emphasis on the reversible V(V)–V(IV) redox couple (Fig. 7**B**). Results listed in Table 2 reveal that as the scan rate (v) was increased from 100 to 500 mV s^{-1}, the peak separation (ΔE_p) became larger, as expected, increasing from 80 to 110 mV, and the ratio of ip_a/ip_c currents is close to 1, indicating reversibility of the studied system. In addition, a plot of the cathodic peak current (I_{pc}) versus $v^{1/2}$ was linear (Fig. 7**C**), revealing that reduction of **2** is a diffusion-controlled process.

For the iron Schiff base complex **3**, the cyclic voltammogram showed a cathodic peak at −0.788 V and an anodic peak at −0.595 mV vs. SCE, which is characteristic of the redox couple Fe (III)/Fe (II) (Fig. 8**A**). The quasi reversibility of the redox couple Fe(III)/Fe(II) is confirmed by the large difference between the anodic and cathodic potentials ($\Delta E_p = Ep_a - Ep_c$), which is greater than 100 mV expected for a transfer of an electron in the reversible system. The cyclic voltammetric behavior was also studied at different scan rates (Fig. 8**B**); results showed that as the scan rate increases, the anodic and cathodic currents increase. In addition, plots of each of the cathodic peak current (I_{pc}) and the anodic current (I_{pa}) versus $v^{1/2}$ was linear (Fig. 8**C**), revealing that reduction of **3** is a diffusion-controlled process.

3.6. Antioxidant activity

3.6.1. Structure/antioxidant activity relationship

In all selected studies reported in the literature, DPPH was selected as free radical because of its ability to be reduced either by a one-electron or by hydrogen atom. Results by Bajju et al. (2019) indicated antioxidant activity of oxovanadium(IV) porphyrin complexes with IC_{50} values between 25 and 40 μg/m. This could be explained by the presence of salicylate and sulfosalicylate groups as an axial ligand in their structures. Moreover, the presence of halides in the structures of the Schiff bases, described by Warad et al. (2020), clearly explained the higher antioxidant activity for these kinds of

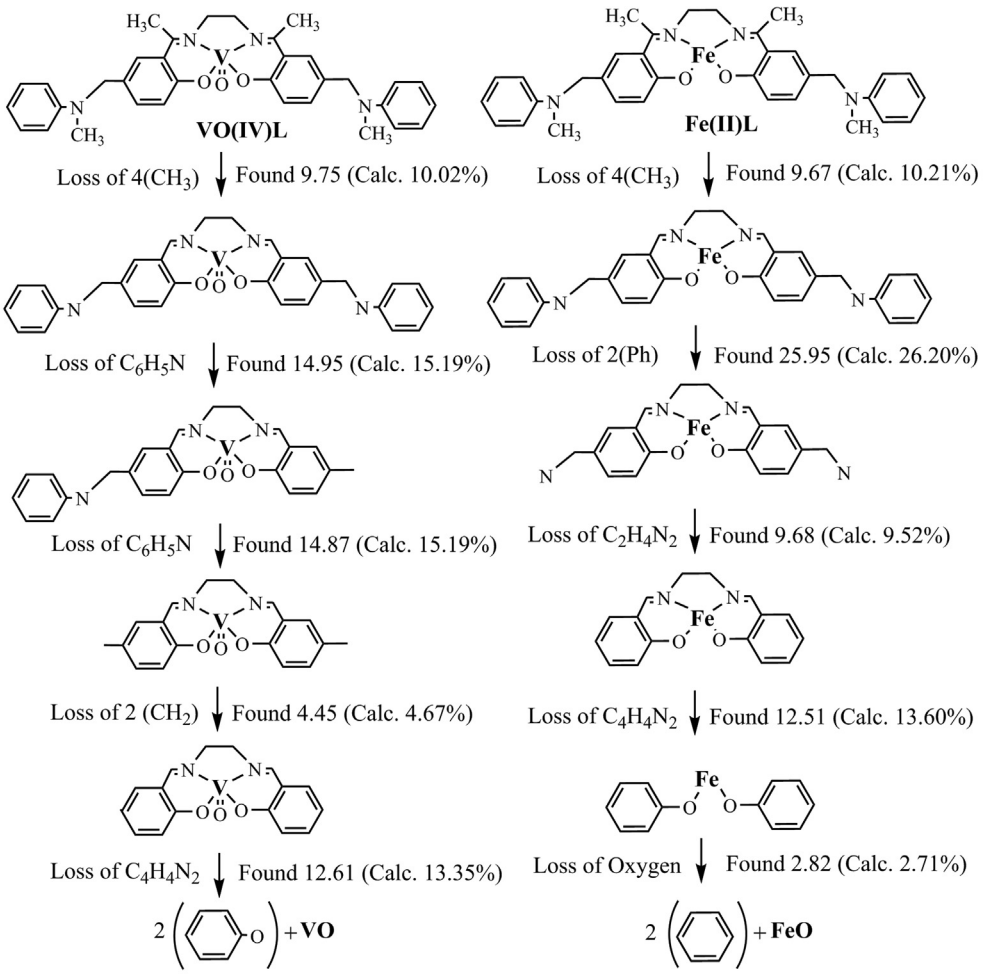

Scheme 3 Decomposition steps with mass loss for the two-oxovanadium and iron complexes obtained from the TG/DTG experiments carried out at 10 °C min^{-1} under a nitrogen atmosphere.

compounds. In addition, the 5-methylpinobanksin ether reported by Rivero-Cruz et al. (2020) showed weaker antioxidant activity compared to other flavonoids. Analysis of their chemical structures was attributed to this weak antioxidant activity of methylated flavonoids.

On the other hand, an iron(III) complex of a Schiff base synthesized from 2,6-diacetylpyridine and glucosamine was investigated by Khalf-Alla et al. (2019). Results indicated that this complex, abbreviated as **$[Fe(dapGH_2)\ (H_2O)_2]^{3+}$** (See Table 3), exhibits high IC_{50} value, which was found to be 394.3 µg/mL. This result is explained on the basis of hydrogen atom donation. In conclusion, examination of the main results of the literature showed that the antioxidant activity increases as phenyl groups are introduced in the structures of these complexes. Inversely, substitution of halides groups in the structures of these kinds of compounds and the nature of the metal ions caused a decrease in the antioxidant activity. Displayed in Table 3 is a list of biological studies carried out by some authors focusing their works on the antioxidant activity using DPPH method. This approach allows comparison of our results with those reported in the literature as shown in Table 3. Our results show that **IC_{50}** values of **VO(IV)L, H_2L,** and **Fe(II)L** are 31.8**,** 373.0**,** and **473.6,** respectively**;** these values are significantly higher than those taken from the literature (**See** Table 3).

3.6.2. Antioxidant activity of H_2L, VO(IV)L, and Fe(II)L

We measured the ability of the synthesized complexes **2** and **3**, along with the Schiff base **H_2L** to donate a hydrogen atom or an electron based on the bleaching of the purple-colored methanol solution of DPPH. DPPH radical absorbs at 517 nm and used as a substrate to evaluate the antioxidant activity. DPPH is frequently used to detect the radical scavenging activity of natural extracts or synthesized compounds due to its stability as a free purple colored radical with an odd electron. In this assay, the color of DPPH disappears when it reacts with an antioxidant. Therefore, the free radical scavenging capacity of the Schiff base ligand and its oxovanadium and iron complexes has been evaluated using this method against ascorbic acid as a positive standard. In these antioxidant tests, the higher activity leads to a lower IC_{50} value; IC_{50} values for **H_2L**, **VO(IV)L**, and **Fe(II)L** were 373.0, 31.8, and, 473.6 µg/mL, respectively. Shown in Fig. 9 and Fig. 10 are results related to the inhibitory effects of the Schiff base and its **VO**

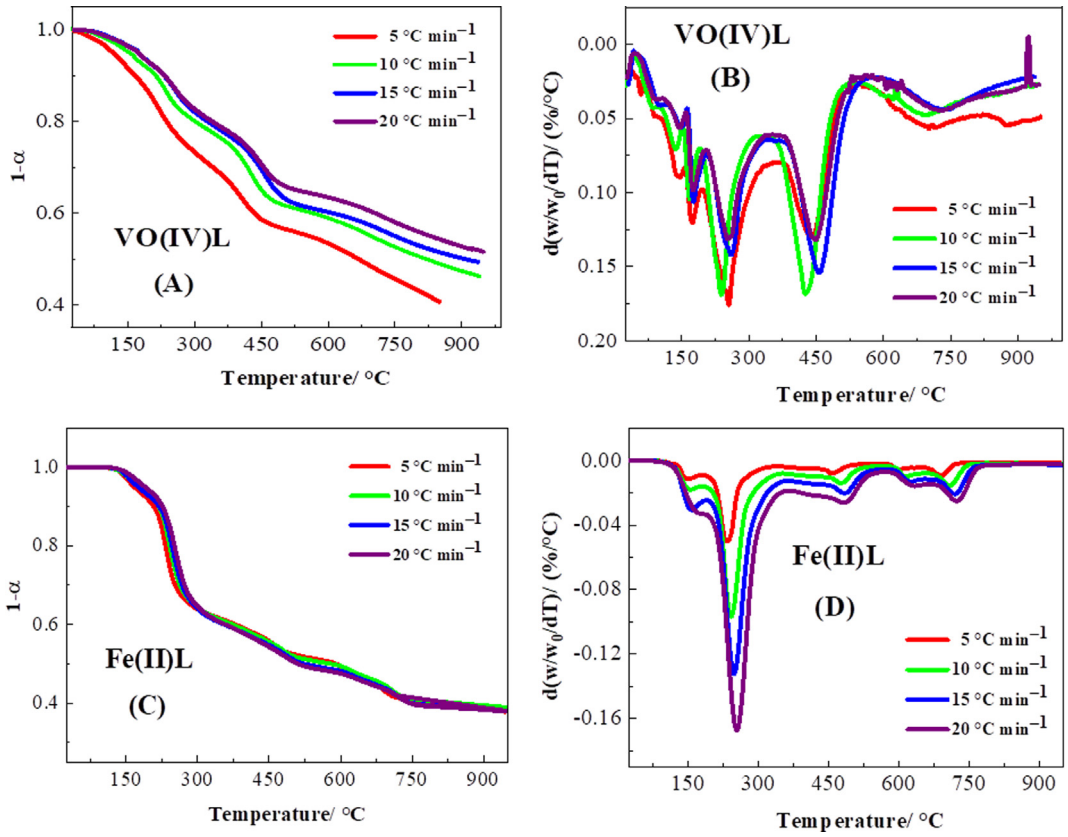

Fig. 5 TG, DTG thermograms of **VO(IV)L** (**A, B**) and **Fe(II)L** (**C, D**) complexes performed at different heating rates of 5, 10, 15 and 20 °C min^{-1} under nitrogen atmosphere.

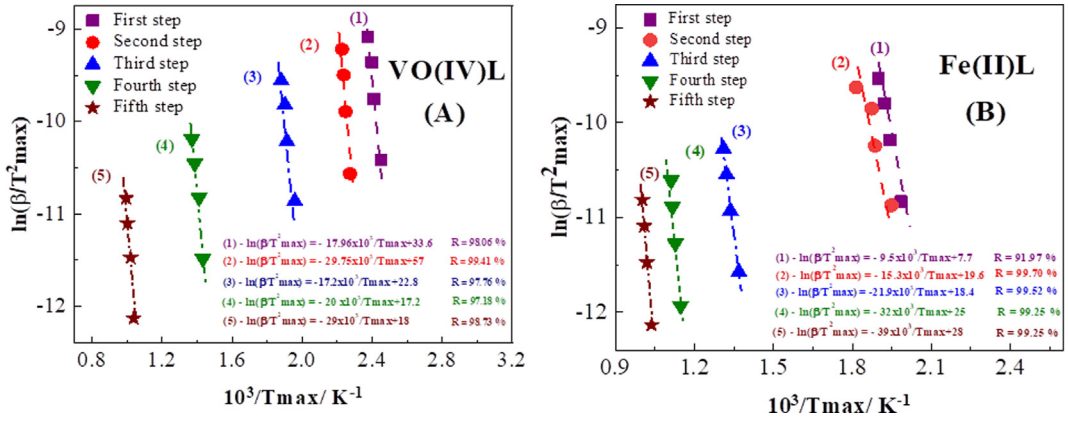

Fig. 6 Kissinger's plots of **VO(IV)L** (**A**) and **Fe(II)L** (**B**) Schiff base complexes performed at different heating rates of 5, 10, 15, and 20 °C min^{-1} under nitrogen atmosphere.

(IV)L and **Fe(II)L** complexes on DPPH. Results revealed that the complex **2** exhibits good activity as a free-radical scavenger in comparison with **1** itself (Pramanik et al., 2015). Our findings show that the prepared compounds exhibit moderate to good antioxidant activities compared to those of the literature (**See** Table 3). The presence of coordinated metal ions changes the structure of the Schiff base, which affects the antioxidant activity. Furthermore, it is possible to draw a conclusion on the relationship between the antioxidant activity and the functional groups present in the complexes. In this respect, substituents in the Schiff base have a great influence on the activity of these compounds (Cheng et al., 2010). Additionally, the antioxidant activity increase by the number of phenyl groups in the complexes (Ghanbari et al., 2014).

Table 1 Kinetic parameters derived from the Kissinger's method.

Samples	T_{max}/°C				Kissinger		
	5	10	15	20	E/ (kJ mol^{-1})	A/s^{-1}	R^2/ %
VO(IV)L	136	142	144	148	149 ± 15	7.0×10^{18}	98.07
	166	170	174	176	247 ± 14	1.7×10^{29}	99.41
	238	250	252	259	143 ± 15	1.4×10^{14}	97.75
	425	439	449	456	166 ± 20	6.1×10^{8}	97.18
	692	708	725	734	242 ± 19	2.0×10^{9}	98.73
Fe(II)L	147	151	156	158	173 ± 20	1.6×10^{21}	97.38
	231	242	247	253	127 ± 5	5.0×10^{9}	99.70
	457	475	484	490	162 ± 9	1.9×10^{9}	99.52
	598	613	624	629	267 ± 13	2.2×10^{12}	99.53
	692	708	718	724	320 ± 3	4.3×101^{9}	99.99

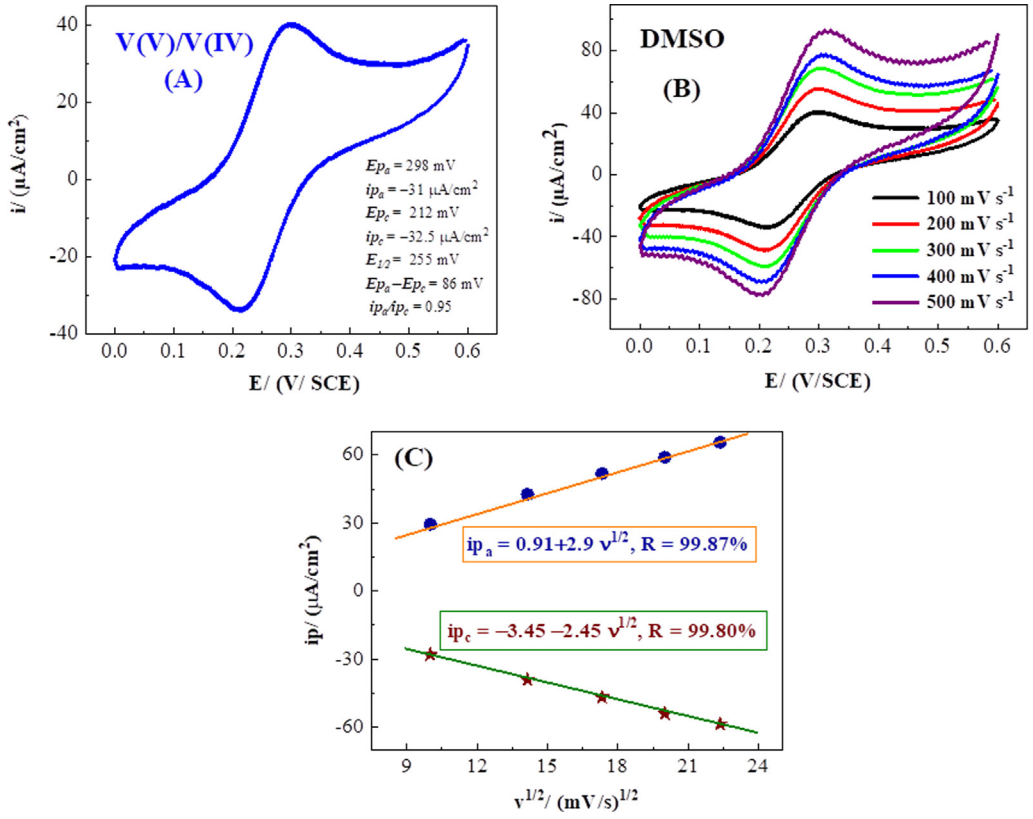

Fig. 7 (**A**) Cyclic voltammograms recorded at 100 mV s^{-1} for reduction of a 1.0 mM solution of the V(V)/V(IV) redox system with a freshly polished glassy carbon electrode) in oxygen-free DMSO containing 0.10 M TBAP. Scan goes from 0.0 to 0.60 to 0.0 V vs. SCE. (**B**) Cyclic voltammograms of the same solution recoded at different scan rates ranging from 100 to 500 mV s^{-1}. (**C**) Plots of anodic (ip_a) and cathodic (ip_c) peak currents versus square root of the scan rate ($\nu^{1/2}$).

4. Conclusions

In summary, we have synthesized two new oxovanadium and iron complexes of the tetradentate N_2O_2 type Schiff base ligand 2,2′-((1E,1′E)-(ethane-1,2-diylbis(azanylylidene))bis(ethan-1-yl-1-ylidene))bis(4-((methyl(phenyl)amino)-methyl)phenol) through reaction with vanadium and iron salts. Structures of these complexes have been determined with the aid of UV–Vis, infrared, and mass spectrometry, and by elemental analysis. The thermal behavior of the two Schiff base complexes of oxovanadium and iron has been investigated by means of TGA and a mechanism of the thermal decomposition has been suggested. In addition, cyclic voltammetry at a glassy carbon cathode in DMSO indicated that each of these complexes exhibits a quasi-reversible wave. Finally, the newly prepared complexes exhibited a moderate to good free radical scavenging

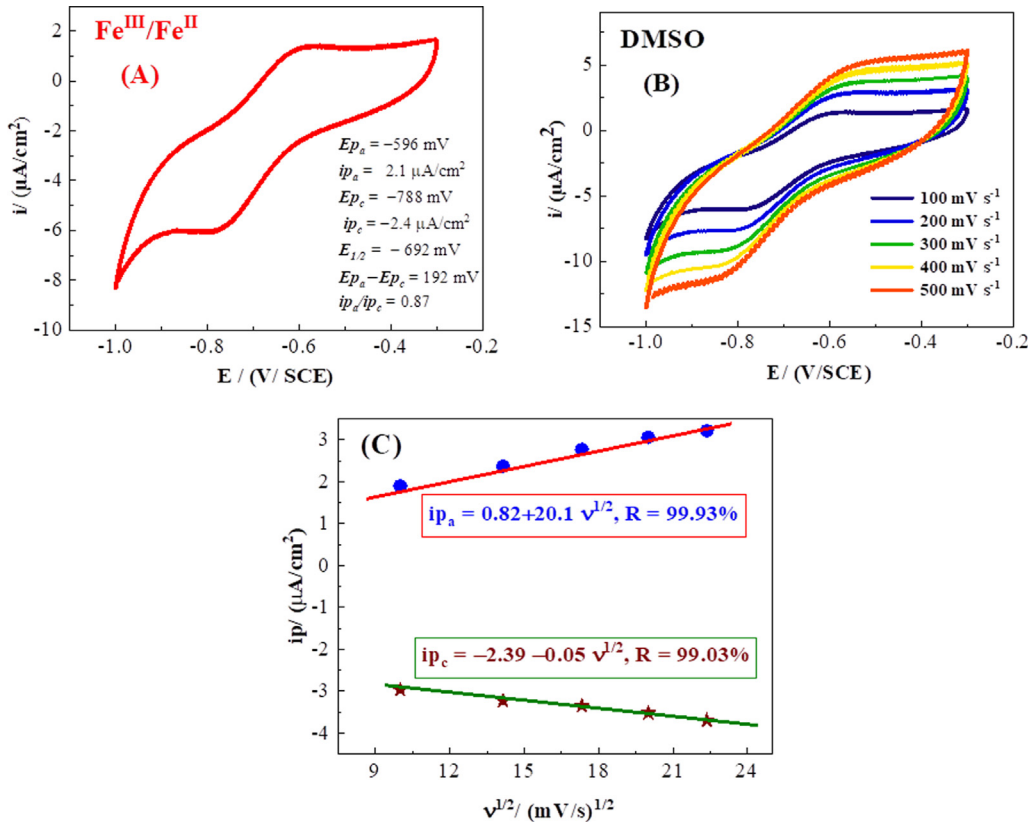

Fig. 8 (**A**) Cyclic voltammograms recorded at 100 mV s^{-1} for reduction of a 1.0 mM solution of the Fe(III)/Fe(II) redox system with a freshly polished glassy carbon electrode) in oxygen-free DMSO containing 0.10 M TBAP. Scan goes from −0.30 to −1.00 V versus SCE. (**B**) Cyclic voltammograms of the same solution recoded at different scan rates ranging from 100 to 500 mV s^{-1}. (**C**) Plots of anodic (ip_a) and cathodic (ip_c) peak currents versus square root of the scan rate ($\nu^{1/2}$).

Table 2 Electrochemical data of oxovanadium(IV) and iron(II) Schiff base complexes at different scan rates.

Samples	Scan rate/(mV s^{-1})	Ep_a/mV	Ep_c/mV	ip_a/(μA cm^{-2})	ip_c/(μA cm^{-2})	ΔEp/mV	$E_{1/2}$/mV	ip_a/ip_c
VO(IV)L	100	291	211	30	−28	80	251	1.04
	200	295	209	43	−39	86	252	1.08
	300	300	207	52	−47	93	254	1.10
	400	306	204	59	−54	102	255	1.08
	500	312	202	66	−59	110	257	1.11
Fe(II)L	100	−596	−788	2	−2	192	692	0.87
	200	−568	−813	2	−3	245	691	0.73
	300	−548	−831	3	−3	283	690	0.82
	400	−534	−849	3	−4	315	692	0.86
	500	−526	−864	3	−4	338	695	0.87

activity, thus they exhibited antioxidant activity. Biological activity has been compared to other structurally related compounds and explanations along with Structure-activity relationships have been provided,

Author's contribution

All authors participated in the formation and design of this study. NM, DA, and HB performed the experimental work, while BB, YO, DL, MG, AO, and MS. M have analyzed and interpreted the data. BB and AO supervised the project. MS. M has critically revised the manuscript. All authors have read and approved the final manuscript.

Declaration of Competing Interest

The authors declare that they have no known competing financial interests or personal relationships that could have appeared to influence the work reported in this paper.

Table 3 Comparison of the IC_{50} (μg/mL) of H_2L, **VO(IV)L**, and **Fe(II)L** with some other studies.

Compounds/Type	IC_{50} (μg/mL)	References
2-(piperazin-1-yl)-N-(thiophen-2-ylmethylene)-ethanamine/***Schiff base ligand***.	12.58	(Warad et al., 2020)
N-(1-(5-chlorothiophen-2-yl) ethylidene)-2-(piperazin-1-yl)ethan amine/**Schiff base ligand**.	5.15	(Warad et al., 2020)
5-methylpinobanksin ether/***Flavonoids***	98.4	(Rivero-Cruz et al., 2020)
Oxovanadium(IV)tetra (4methoxyphenyl)porphyrinsalicylate or -sulphosalicylate/***Oxovanadium complex***	25.0 and 40.0	(Bajju et al., 2019)
$[Fe\ (dapGH_2)(H_2O)_2]^{3+}$/***Iron complex***	394.3	(Khalf-Alla et al., 2019)
H_2L/Schiff base ligand	373.0	**This work**
VO(IV)L/Oxovanadium complex	31.8	**This work**
Fe(II)L/Iron complex	473.6	**This work**

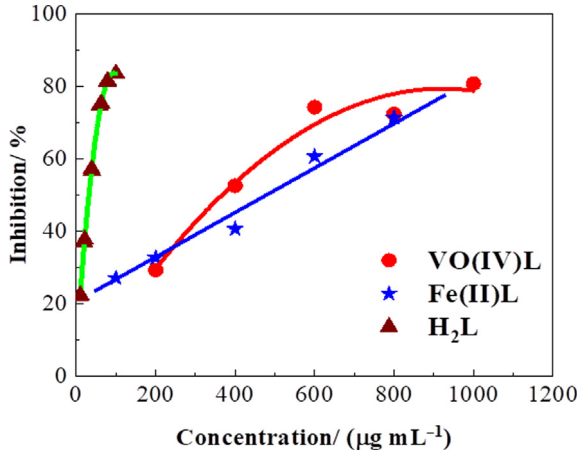

Fig. 9 DPPH radical-scavenging activities of H_2L, **VO(IV)L**, and **Fe(II)L**.

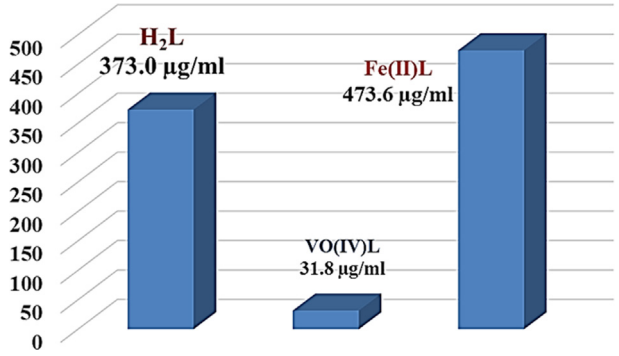

Fig. 10 IC_{50} inhibitory concentration of ligand and its oxovanadium and iron complexes for 50% of DPPH radical.

Acknowledgements

Authors thank the Algerian Ministry of Higher Education and Scientific Research (MESRS) and the Director General for Scientific Research and Technological Development (DGRSDT) for financial support. Authors also extend their thanks and appreciation to the Emerging Materials Research Unit (URMES) of Ferhat ABBAS Setif-1 University for carrying out thermogravimetric analyses.

References

Abdallah, S.M., Zayed, M.A., Mohamed, G.G., 2010. Synthesis and spectroscopic characterization of New tetradentate Schiff base and its coordination compounds of NOON donor atoms and their antibacterial and antifungal activity. Arab. J. Chem. 3, 103–113.

Abd El-Halim, H.F., Anwar, M.N., Mohamed, G.G., 2017. Antimicrobial and anticancer activities of Schiff base ligand and its transition metal mixed ligand complexes with heterocyclic base. Appl. Organomet. Chem. 32, e 3899.

Abd El-Rahman, L.H., Abu-Dief, A.M., Moustafa, H., Abdel-Mawgoud, A.A.H., 2020. Design and nonlinear optical properties (NLO) using DFT approach of new Cr(III), VO(II), and Ni(II) chelates incorporating tri-dentate imine ligand for DNA interaction, antimicrobial, anticancer activities and molecular docking studies. Arab. J. Chem. 13, 649–670.

Abd El-Rahman, L.H., El-Khatib, R.M., Nassr, L.A.E., Abu-Dief, A. M., 2017. DNA binding ability mode, spectroscopic studies, hydrophobicity, and in vitro antibacterial evaluation of some new Fe(II) complexes bearing ONO donors amino acid Schiff bases. Arab. J. Chem. 10, S1835–S1846.

Aggoun, D., Ourari, A., Ruiz-Rosas, R., Morallon, E., 2017. A selective naked-eye chemosensor derived from 2-methoxybenzylamine and 2,3-dihydroxybenzaldehyde: synthesis, spectral characterization and electrochemistry of its bis-bidentates Schiff bases metal complexes. Spectrochim. Acta A. 184, 299–307.

Al-Obiadi, O.H.S., 2012. Synthesis, characterization and theoretical treatment of sandwich Schiff bases complexes derived from salicylaldehyde with some transition metals and study of its biological activity. Int. J. Chem. Res. 3, 1–5.

Al Zoubi, W., Al-Hamdani, A.A.S., Ahmed, S.D., Ko, Y.G., 2017. Synthesis, characterization, and biological activity of Schiff bases metal complexes. J. Phys. Org. Chem. 31, e3752.

Anthonysamy, A., Balasubramanian, S., 2005. Synthesis, spectral, thermal and electrochemical studies of nickel (II) complexes with N_2O_2 donor ligands. Inorg. Chem. Commun. 8, 908–911.

Asadi, M., Asadi, Z., Savaripoor, N., Dusek, M., Eigner, V., Shorkaei, M.R., Sedaghat, M., 2015. Structural investigation of oxovanadium(IV) Schiff base complexes: X-ray crystallography, electrochemistry and kinetic of thermal decomposition. Spectrochim. Acta Part A. 136, 625–634.

Bagherzadeh, M., Amini, M., 2009. Synthesis, characterization and catalytic study of a novel iron(III)- tridentate Schiff base complex in sulfide oxidation by UHP. Inorg. Chem. Commun. 12, 21–25.

Bagherzadeh, M., Amini, M., 2010. A new vanadium Schiff base complex as catalyst for oxidation of alcohols. J. Coord. Chem. 63, 3849–3858.

Bajju, G.D., Ahmed, A.A., Devi, G., 2019. Synthesis and bioactivity of oxovanadium(IV)tetra (4-methoxyphenyl) porphyrinsalicylates. BMC Chem. 13, 15.

Basak, T., Ghosh, K., Chattopadhyay, S., 2018. Synthesis, characterization and catechol oxidase mimicking activity of two iron(III) Schiff base complexes. Polyhedron 146, 81–92.

Bikas, R., Hosseini-Monfared, H., Jeanneau, E., Shaabani, B., 2013. Synthesis, structural characterization and electrochemical studies of new oxovanadium(v) complexes derived from 2- furanoylhydrazon derivatives. J. Chem. 2013, 1–12.

Blois, M.S., 1958. Antioxidant determinations by the use of a stable free radical. Nature 181, 1199–1200.
Ghanbari, Z., Housaindokht, M.R., Izadyar, M., Bozorgmehr, M.R., Eshtiagh-Hosseini, H., Bahrami, A.R., Matin, M.M., Khoshkholgh, M.J., 2014. Structure-activity relationship for Fe(III)-Salen-like complexes as potent anticancer agents. Sci. World J. 2014, 745649.
Cheng, L.X., Tang, J.J., Luo, H., Jin, X.L., Dai, F., Yang, J., Qian, Y. P., 2010. Antioxidant and antiproliferative activities of hydroxyl-substituted Schiff bases. Bioorg. Med. Chem. Lett. 8, 2417–2420.
Conley, R.T., 1966. Infrared Spectroscopy. Allyn and Bacon, Boston, Mass, USA.
De Fátima, A., Pereira, C.P., Olímpio, C.R.S.D.G., de Freitas Oliveira, B.G., Franco, L.L., da Silva, P.H.C., 2018. Schiff bases and their metal complexes as urease inhibitors a brief review. J. Adv. Res. 13, 113–126.
Elmali, A., Karakas, A., Unver, H., 2005. Nonlinear optical properties of bis[(*p*-bromophenyl-salicylaldiminato) chloro]iron(III) and its ligand N-(4-bromo)-salicylaldimine. Chem. Phys. 309, 251–257.
El-Shafiy, H.F., Shebl, M., 2019. Binuclear oxovanadium(IV), cerium (III) and dioxouranium(VI) nanocomplexes of a bis(bidentate) ligand: Synthesis, spectroscopic, thermal, DFT calculations and biological studies. J. Mol. Struct. 1194, 187–203.
Elsayed, S.A., Noufal, A.M., El-Hendawy, A.M., 2017. Synthesis, structural characterization and antioxidant activity of some vanadium(IV), Mo(VI)/(IV) and Ru(II) complexes of pyridoxal Schiff base derivatives. J. Mol. Struct. 1144, 120–128.
Ghazizadeh, M., Badiei, A., Sheikhshoaie, I., 2017. Iron-functionalized nanoporous silica type SBA-15: Synthesis, characterization and application in alkene epoxidation in presence of hydrogenperoxide. Arab. J. Chem. 10, S2491–S2498.
Gorczyński, A., Pakulski, D., Szymańska, M., Kubicki, M., Bułat, K., Łuczak, T., Patroniak, V., 2016. Electrochemical deposition of the new manganese(II) Schiff-base complex on a gold template and its application for dopamine sensing in the presence of interfering biogenic compounds. Talanta. 149, 347–355.
Han, H., Lu, L., Wang, Q., Zhu, M., Yuan, C., Xing, S., Fu, X., 2012. Synthesis and evaluation of oxovanadium(IV) complexes of Schiff-base condensates from 5-substituted-2- hydroxybenzaldehyde and 2 substituted benzenamine as selective inhibitors of protein tyrosine phosphatase 1B. Dalton Trans. 41, 11116–11124.
Hassan, M., Nasr, S.M., Abd-El-Razek, S.E., Abdel-Aziz, M.S., El-Gamasy, S.M., 2020. New superior bioactive metal complexes of ligand with N, O donor atoms bearing sulfadiazine moiety: Physicochemical study and thermal behavior for chemotherapeutic application. Arab. J. Chem. 13, 7324–7337.
Jacob, M., Bhattacharya, P.K., Ganeshpure, P.A., Satish, S., Sivaram, S., 1989. Epoxidation of alkenes catalyzed by iron(III) Schiff base chelates. A monooxygenase model. Bull. Chem. Soc. Jpn. 62, 1325–1327.
Khalf-Alla, P.A., Hassan, S.S., Shoukry, M.M., 2019. Complex formation equilibria, DFT, docking, antioxidant and antimicrobial studies of iron(III) complexes involving Schiff bases derived from glucosamine or ethanolamine. Inorg. Chim. Acta. 492, 192–197.
Kianfar, A.H., Mohebbi, S., 2007. Synthesis and Electrochemistry of vanadium(IV) Schiff Base complexes. J. Iran. Chem. Soc. 4, 215–220.
Kissinger, H.E., 1957. Reaction kinetics in differential thermal analysis. Anal. Chem. 21, 1702–1706.
Kolawole, G., Patel, K.S., 1981. The stereochemistry of oxo-vanadium (IV) complexes derived from salicylaldehyde and polymethylene diamines. J. Chem. Soc. Dalton Trans., 1241–1245
Lu, L., Yue, J., Yuan, C., Zhu, M., Han, H., Liu, Z., Guo, M., 2011. Ternary oxovanadium(IV) complexes with amino acid-Schiff base and polypyridyl derivatives: Synthesis, characterization, and protein tyrosine phosphatase 1B inhibition. J. Inorg. Biochem. 105, 1323–1328.
Mahalakshmi, N., Rajavel, R., 2014. Synthesis, spectroscopic, DNA cleavage and antibacterial activity of binuclear Schiff base complexes. Arab. J. Chem. 7, 509–517.
Mahroof-Tahir, M., Brezina, D., Fatima, N., Choudhary, M.I., Tahman, A., 2005. Synthesis and characterization of mononuclear oxovanadium(IV) complexes and their enzyme inhibition studies with a carbohydrate metabolic enzyme phosphodiesterase. I. J. Inorg. Biochem. 99, 589–599.
Manjula, B., Arul, S., 2013. Preparation, characterization, antimicrobial activities and DNA cleavage studies of Schiff base complexes derived from 4-amino antipyrine. Asian J. Biochem. Pharm. Res. 1, 168–178.
Maurya, M.R., Khurana, S., Shailendra, Azam, A., Zhang, W., Rehder, D., 2003. Synthesis, characterisation and antiamoebic studies of dioxovanadium(V) complexes containing ONS donor ligands derived from S-benzyldithiocarbazate. Eur. J. Inorg. Chem. 2003, 1966−1973.
Maurya, R.C., Sutradhar, D., Martin, M.H., Roy, S., Chourasia, J., Sharma, A.K., Vishwakarma, P., 2015. Oxovanadium(IV) complexes of medicinal relevance: Synthesis, characterization, and 3D-molecular modeling and analysis of some oxovanadium(IV) complexes in O, N-donor coordination matrix of sulfa drug Schiff bases derived from a 2-pyrazolin-5-one derivative. Arab. J. Chem. 8, 78–92.
Melchior, M., Thompson, K.H., Jong, J.M., Rettig, S.J., Shuter, E., Yuen, V.G., Zhou, Y., Neill, J.H.M., Orvig, C., 1999. Vanadium complexes as insulin mimetic agents: Coordination chemistry and in vivo studies of oxovanadium(IV) and dioxovanadate(V) complexes formed from naturally occurring chelating oxazolinate, thiazolinate, or picolinate units. Inorg. Chem. 38, 2288–2293.
Miloud, M.M., El-ajaily, M.M., Al-noor, T.H., Al-barki, N.S., 2020. Antifungal activity of some mixed ligand complexes incorporating Schiff bases. J. Bacteriol. Mycol. 7, 1122.
Murtaza, G., Mumtaz, A., Khan, F.A., Ahmad, S., Azhar, S., Najam-Ul-Haq, M., Atif, M., Khan, S.A., Maalik, A., Alam, F., Hussain, I., 2014. Recent pharmacological advancements in Schiff bases: A review. Acta Pol. Pharm. 71, 531–535.
Ouennoughi, Y., Karce, H.E., Aggoun, D., Lanez, T., Ruiz-Rosas, R., Bouzerafa, B., Ourari, A., Morallon, E., 2017. Novel Ferrocenic Copper II complex salen-like, derived from 5-chloromethyl- 2-hydroxyacetophenone and n-ferrocenmethyl aniline: Design, spectral approach and solvent effect towards electrochemical behavior of Fc^{+}/Fc redox couple. J. Organomet. Chem. 848, 344–351.
Ourari, A., Khelafi, M., Aggoun, D., Jutand, A., Amatore, C., 2012. Electrocatalytic oxidation of organic substrates with molecular oxygen using tetradentate ruthenium(III)-Schiff base complexes as catalysts. Electrochim. Acta. 75, 366–370.
Ourari, A., Ouennoughi, Y., Aggoun, D., Mubarak, M.S., Pasciak, E. M., Peters, D.G., 2014. Synthesis, characterization, and electrochemical study of a new tetradentate nickel(II)-Schiff base complex derived fromethylenediamine and 5′-(*N*-methyl-*N*-phenylaminomethyl)-2'- hydroxyacetophenone. Polyhedron 67, 59–64.
Ourari, A., Messali, S., Bouzerafa, B., Ounnougui, Y., Aggoun, D., Mubarak, M.S., Strawsine, L.M., Peters, D.G., 2015. Synthesis, characterization, and electrochemical behavior of a cobalt(II) salen- like complex. Polyhedron 97, 197–201.
Pawar, V., Joshi, S., Uma, V., Prakash, B., Joshi, S.C., 2013. Template synthesis and pharmacological properties of oxovanadium (IV) complexes of macrocyclic Schiff bases. Int. J. Pharm. Sci. Rev. Res. 19, 21–26.
Percy, G.C., Thornton, D.A., 1972. N-alkyl salicylaldimine complexes: infrared and PMR spectra of the ligands and vibrational frequencies of their metal(II) chelates. J. Inorg. Nucl. Chem. 34, 3369–3376.
Prakach, A., Adhikari, D., 2011. Application of Schiff bases and their metal complexes-A review. Int. J. Chem. Tech. Res. 3, 1891–1896.
Pramanik, H.A.R., Paul, P.C., Mondal, P., Bhattacharjee, C.R., 2015. Mixed ligand complexes of cobalt(III) and iron(III) containing

N_2O_2-chelating Schiff base: Synthesis, characterization, antimicrobial activity, antioxidant and DFT study. J. Mol. Struct. 1100, 496–505.

Ramadhan, U.H., Haddad, H.M., Ezaria, Z.G., 2016. Synthesis of Schiff bases complexes as anti- inflammatory agents. World J. Pharm. Pharm. Sci. 5, 98–108.

Rani, S., Bhat, B.R., 2010. Effective oxidation of alcohols by iron(III)-Schiff base-triphenylphosphine complexes. Tetrahedron Lett. 51, 6403–6405.

Rayati, S., Ashouri, F., 2012. Pronounced catalytic activity of oxovanadium(IV) Schiff base complexes in the oxidation of cyclooctene and styrene by *tert*-butylhydroperoxide. C. R. Chim. 15, 679–687.

Rivero-Cruz, J.F., Granados-Pineda, J., Pedraza-Chaverri, J., Pérez-Rojas, J.M., Kumar-Passari, A., Diaz-Ruiz, G., Rivero-Cruz, B.E., 2020. Phytochemical constituents, antioxidant, cytotoxic, and antimicrobial activities of the ethanolic extract of Mexican brown propolis. Antioxidants 9, 70.

Sasmal, P.K., Patra, A.K., Chakravarty, A.R., 2008. Synthesis, structure, DNA binding and DNA cleavage activity of oxovanadium(IV) N-salicylidene-S-methyldithiocarbazate complexes of phenanthroline bases. J. Inorg. Biochem. 102, 1463–1472.

Shi, S., Yu, S., Quan, L., Mansoor, M., Chen, Z., Hu, H., Liu, D., Liang, Y., Liang, F., 2020. Synthesis and antitumor activities of transition metal complexes of a bis-Schiff base of 2-hydroxy-1-naphthalenecarboxaldehyde. J. Inorg. Biochem. 210, 111173.

Schiff, H., 1869. Untersuchungen über Salicin derivate. Ann. Chem. 150, 193–200.

Shukla, S., Mishra, A.P., 2019. Metal complexes used as anti-inflammatory agents: Synthesis, characterization and anti-inflammatory action of VO(II)-complexes. Arab. J. Chem. 12, 1715–1721.

Sungh, B.K., Mishra, P., Prakash, A., Bhojak, N., 2017. Spectroscopic, electrochemical and biological studies of the metal complexes of the Schiff base derived from pyrrole-2-carbaldehyde and ethylenediamine. Arab. J. Chem. 10, S472–S483.

Surati, K.R., Sathe, P.A., 2016. Schiff base pyrazolone complexes of iron (III): synthesis, characterization, antimicrobial and antioxidant activity. Med. Chem. Res. 25, 2742–2751.

Uddin, N., Rashid, F., Ali, S., Tirmizi, S.A., Ahmad, I., Zaib, S., Zubair, M., Diaconescu, P.L., Tahir, M.N., Iqbal, J., Haider, A., 2020. Synthesis, characterization, and anticancer activity of Schiff bases. J. Biomol. Struct. Dyn. 38, 3246–3259.

Vairalakshmi, M., Princess, R., 2019. Metal complexes of novel Schiff base containing isatin: Characterization, antimicrobial, antioxidant and catalytic activity study. Asian J. Pharm. Clin. Res. 12, 206–210.

Warad, I., Ali, O., Al Ali, A., Jaradat, N.A., Hussein, F., Abdallah, L., Al-Zaqri, N., Alsalme, A., Alharthi, F.A., 2020. Synthesis and spectral identification of three Schiff bases with a 2-(piperazin-1-yl)-n-(thiophen-2-yl methylene)ethanamine moiety acting as novel pancreatic lipase inhibitors: Thermal, DFT, antioxidant, antibacterial, and molecular docking investigations. Molecules 25, 2253.

Yaul, A., Pethe, G., Deshmukh, R., Aswar, A., 2013. Vanadium complexes with quadridentate Schiff bases: Synthesis, characterization, thermal and catalytic studies. J. Therm. Anal. Cal. 113, 745–752.

Zayed, E.M., Zayed, M.A., Hindy, A.M.M., 2014. Thermal and spectroscopic investigation of novel Schiff base, its metal complexes, and their biological activities. J. Therm. Anal. Cal. 116, 391–400.